Proceedings of the CERN-BINP Workshop for Young Scientists in e^+e^- Colliders, Geneva, Switzerland, 22 – 25 August 2016, edited by V. Brancolini ans L. Linssen, CERN Proceedings, Vol. 1/2017, CERN-Proceedings-2017-001 (CERN, Geneva, 2017)

Towards an Optimized Monochromatization for Direct Higgs Production in Future Circular e^+e^- Colliders

M.A. Valdivia García[*1,2] *and F. Zimmermann*[1,2]
CERN, Geneva, Switzerland
University of Guanajuato, Mexico

Abstract

Direct s-channel Higgs production in e^+e^- collisions is of interest if the centre-of-mass energy spread can be reduced to be comparable to the width of the standard model Higgs boson. A monochromatization principle, previously proposed for several earlier lower-energy colliders, could be employed to achieve the desired reduction, by introducing a non-zero horizontal dispersion of opposite sign for the two colliding beams at the interaction point. In high-energy, high-luminosity circular colliders, beamstrahlung may increase the energy spread and bunch length. Horizontal emittance increase due to beamstrahlung, a new effect that was not present in past monochromatization proposals, may degrade the performance, especially the luminosity. We study, for the FCC-ee collider at 62.5 GeV beam energy, how to optimize the interaction point optics parameters (β_x^*, D_x^*), along with the number of particles per bunch, so as to obtain maximum luminosity at a desired target value of the collision energy spread.

Keywords

Monochromatization; beamstrahlung; collider; high energy; high luminosity; storage ring.

1 Introduction

Monochromatization is a technique that was proposed several decades ago to reduce the centre-of-mass energy spread at e^+e^- colliders [1], but has never been used in any operational collider. A decrease in collision energy spread σ_ω can be accomplished without reducing the inherent energy spread σ_ϵ of either of the two colliding beams. To achieve this goal, opposite correlations between spatial position and energy are introduced at the interaction point (IP). In beam-optical terms, this can be accomplished through a non-zero dispersion function for both beams of opposite sign at the IP. The dispersion is determined by the respective lattice [2].

The concept of monochromatic collision allows for an interesting option presently under study for the FCC-ee collider [3,4], namely the possibility of direct Higgs production in the s channel, $e^+e^- \to H$, at a beam energy of 62.5 GeV. This could result in an acceptable Higgs event rate on the Higgs resonance and also provide the energy precision required to measure the width of the Higgs particle [5].

Implementation of a monochromatization scheme has been explored for several colliders in the past [1,2,6–11], but, to our knowledge, no such a scheme has ever been applied, or tested, in any operating collider.

The FCC-ee collider design considers two horizontally separated rings for electrons and positrons. For such a double ring collider, where the two beams circulate in separate beam pipes with independently powered magnets, it will be rather simple to modify the dispersion function for the two beams independently. In particular, a horizontal dispersion at the IP could be generated with opposite sign for the two

[*] valdivia@fisica.ugto.mx and alan.valdivia@cern.ch

https://doi.org/10.23727/CERN-Proceedings-2017-001.1

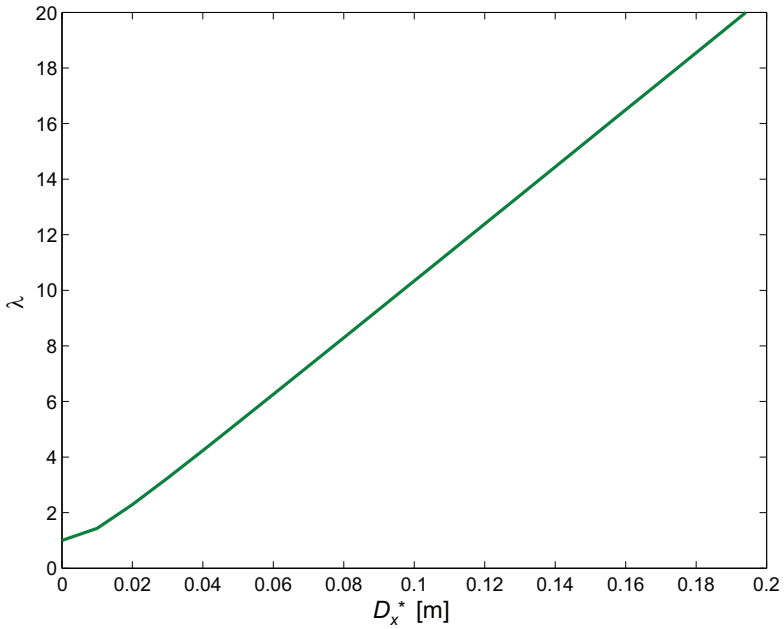

Fig. 1: Monochromatization factor versus D_x^* at fixed $\beta_x^* = 0.25\,\mathrm{m}$, for constant emittance and energy spread, equal to $\sigma_\delta = 0.06$ and $\epsilon_x = 0.17\,\mathrm{nm}$.

beams. The impact of this monochromatization on the luminosity and energy spread must be analysed, taking into account the effect of beamstrahlung.

2 Monochromatization principle

For a standard collision, the centre-of-mass energy $W = E_{\mathrm{b}^+} + E_{\mathrm{b}^-} = 2E_{\mathrm{b}}$, with relative spread $\Sigma_w = \sigma_w/W$, is a factor of $\sqrt{2}$ less than than the r.m.s. relative beam energy spread $\sigma_w = \sqrt{\sigma_{\delta^+}^2 + \sigma_{\delta^-}^2} = \sqrt{2}\sigma_\delta$, namely:

$$(\Sigma_w)_{\mathrm{standard}} = \frac{\sigma_\delta}{\sqrt{2}}\,. \tag{1}$$

In a monochromatic collision, we introduce IP dispersion of opposite sign for the two beams, so that particles with energy $E + \Delta E$ collide on average with particles of energy $E - \Delta E$ and the spread in the centre-of-mass energy is reduced by the monochromatization factor λ,

$$\mathrm{stable}\,(\Sigma_w)_\lambda = \frac{\sigma_\delta}{\sqrt{2}}\frac{1}{\lambda}\,, \tag{2}$$

where this factor is defined, for a horizontal IP dispersion $D_{x_+}^* = -D_{x_-}^* \neq 0$ and a vertical IP dispersion $D_{y_+}^* = D_{y_-}^* = 0$, by

$$\lambda = \sqrt{\frac{D_x^{*2}\sigma_\delta^2}{\epsilon_x\beta_x^*} + 1}\,. \tag{3}$$

Figure 1 illustrates the dependence of the monochromatization factor λ on the IP dispersion D_X^*, for fixed relative energy spread σ_δ and horizontal emittance ϵ_x.

In practice, beamstrahlung affects the values of σ_δ and ϵ_x, and its effects will be included in the subsequent analysis.

3 Beamstrahlung

When charged particles pass through the magnets of a storage ring, synchrotron radiation is emitted as a discrete random process, producing statistically independent discrete changes in the energy of the charged particle. For the beam particles, the cumulative effect of the energy loss introduces a noise excitation of the longitudinal and transverse oscillations, causing their amplitudes to increase until they are balanced, on average, by the radiation damping. This damping depends only on the average rate of emission of energy and not on any of its other statistical properties, whereas the excitation is due to the fluctuation of the radiation about its average rate.

A different type of synchrotron radiation, known as beamstrahlung [12–16], is encountered during the interaction with the opposite beam. For short bunch lengths and small transverse beam sizes, the effective bending radius due to the field of the opposing bunch is exceptionally small compared with the typical arc bending radius. At high collision energies, especially for extremely small bunches where the classical critical photon energy during the collision becomes comparable to the beam energy [16], a quantum mechanical description of the radiation process is necessary.

3.1 Describing the radiation

Synchrotron radiation from charged particles is emitted over a typical time interval of order $\rho/(\gamma c)$, where ρ denotes the radius of curvature of a particle trajectory, c the speed of light, and γ the relativistic Lorentz factor. This time can normally be considered instantaneous compared with the betatron and synchrotron oscillation periods.

The strength of the beamstrahlung is characterized by the parameter Υ, defined as [15, 16] $\Upsilon \equiv B/B_\mathrm{c} = (2/3)\hbar\omega_\mathrm{c}/E_\mathrm{e}$, with $B_\mathrm{c} = m_\mathrm{e}^2 c^2/(e\hbar) \approx 4.4\,\mathrm{GT}$, the Schwinger critical field, ω_c the critical energy as defined by Sands [17], and E_e the electron energy before radiation. If the energy of an emitted photon is a few per cent of its initial energy, the emitting particle may fall outside of the momentum acceptance and be lost.

For the collision of Gaussian bunches with r.m.s. sizes σ_x, σ_y, and σ_z, the peak and average values of Υ are given by [16]

$$\Upsilon_\mathrm{max} = 2\frac{r_\mathrm{e}^2\gamma N_\mathrm{b}}{\alpha\sigma_z(\sigma_x^* + \sigma_y^*)}\,, \qquad \text{and} \qquad \Upsilon_\mathrm{ave} \approx \frac{5}{6}\frac{r_\mathrm{e}^2\gamma N_\mathrm{b}}{\alpha\sigma_z(\sigma_x^* + \sigma_y^*)}\,, \tag{4}$$

where α denotes the fine structure constant, $\alpha \approx 1/137$, and r_e the classical electron radius; $r_\mathrm{e} \approx 2.8 \times 10^{-15}\,\mathrm{m}$.

The general emission rate spectrum (photons emitted per second per energy interval) of this radiation is described by [16]

$$\frac{\mathrm{d}W_\gamma}{\mathrm{d}\omega\hbar} = \frac{\alpha}{\sqrt{3}\hbar\pi\gamma^2}\left(\int_\xi^\infty K_{5/3}(\xi')\mathrm{d}\xi' + \frac{y^2}{1-y}K_{2/3}(\xi)\right)\,, \tag{5}$$

where $y \equiv \omega/E_\mathrm{e}$ and $\xi \equiv (2/3)(\omega/\Upsilon(E - \hbar\omega)$ have been introduced. In the classical regime ($\Upsilon \to 0$), this reduces to the well-known expression [17]

$$\left(\frac{\mathrm{d}W_\gamma}{\mathrm{d}\omega\hbar}\right)_\mathrm{classical} = \frac{\alpha}{\sqrt{3}\pi\gamma^2}\int_\xi^\infty K_{5/3}(\xi')\mathrm{d}\xi'\,. \tag{6}$$

The number of photons radiated per unit time is obtained by integrating over ω:

$$\frac{\mathrm{d}N_\gamma}{\mathrm{d}t} = \int_0^{E_\mathrm{e}/\hbar}\frac{\mathrm{d}W_\gamma}{\mathrm{d}\omega}\,\mathrm{d}\omega\,. \tag{7}$$

The number of photons emitted during a single collision can be obtained by integrating Eq. (7) over time and averaging over the bunch distribution, taking into account the variation of Υ. The result for head-on collision of Gaussian bunches has been derived previously [16].

All proposed high-energy circular colliders operate in a parameter region where $\Upsilon \ll 1$ and $\sigma_x \gg \sigma_y$, implying that in this case we can approximate the average number of photons per collision as [16]

$$n_\gamma \approx \frac{12}{\pi^{3/2}} \frac{\alpha r_\mathrm{e} N_\mathrm{b}}{\sigma_x + \sigma_y} \approx \frac{12}{\pi^{3/2}} \frac{\alpha r_\mathrm{e} N_\mathrm{b}}{\sigma_x} \,, \tag{8}$$

and the average relative energy loss as

$$\delta_\mathrm{B} \approx \frac{24}{3\sqrt{3}\pi^{3/2}} \frac{r_\mathrm{e}^3 \gamma N_\mathrm{b}^2}{\sigma_z (\sigma_x + \sigma_y)^2} \approx \frac{24}{3\sqrt{3}\pi^{3/2}} \frac{r_\mathrm{e}^3 \gamma N_\mathrm{b}^2}{\sigma_z \sigma_x^2} \,. \tag{9}$$

The average photon energy normalized to the beam energy $\langle u \rangle$, i.e., the ratio of δ_B and n_γ, is given by

$$\langle u \rangle = \frac{\delta_\mathrm{B}}{n_\gamma} \approx \frac{2\sqrt{3}}{9} \frac{r_\mathrm{e}^2 N_\mathrm{b} \gamma}{\alpha \sigma_z \sigma_x} \,. \tag{10}$$

In the classical regime, the average squared photon and the average photon energies are related via [17]

$$\langle u^2 \rangle \approx \frac{25 \times 11}{64} \langle u \rangle^2 \,. \tag{11}$$

Noting that, in the general case,

$$\langle u \rangle \propto \int_0^{E_\mathrm{e}} \omega (\mathrm{d}W_\gamma / \mathrm{d}\omega) \mathrm{d}\omega \,, \qquad \langle u^2 \rangle \propto \int_0^{E_\mathrm{e}} \omega^2 (\mathrm{d}W_\gamma / \mathrm{d}\omega) \mathrm{d}\omega \,, \tag{12}$$

we can use the general photon distributions of Eq. (5) to examine the applicability of this relation as a function of Υ. The validity of Eq. (11) up to $\Upsilon \sim 10^{-3}$ is illustrated in Fig. 2.

The excitation term $\{n_\gamma \langle u^2 \rangle\}$ for a single collision will be required in the following. According to Eqs. (8) and (11), for small Υ this can be written as

$$n_\gamma \langle u^2 \rangle \approx 1.4 \, \frac{r_\mathrm{e}^5 N_\mathrm{b}^3 \gamma^2}{\alpha \sigma_z^2 (\sigma_x + \sigma_y)^3} \approx 192 \, \frac{r_\mathrm{e}^5 N_\mathrm{b}^3 \gamma^2}{\sigma_z^2 \sigma_x^3} \,. \tag{13}$$

3.2 Energy loss and damping time

The longitudinal damping time in the presence of beamstrahlung is

$$\tau_{E,\mathrm{tot}} = \frac{T_\mathrm{rev} E_\mathrm{beam}}{U_{0,\mathrm{SR}} + n_\mathrm{IP} U_{0,\mathrm{BS}}} \approx \tau_{E,\mathrm{SR}} \left(1 - n_\mathrm{IP} \frac{U_{0,\mathrm{BS}}}{U_{0,\mathrm{SR}}} \right) \,, \tag{14}$$

where T_rev denotes the revolution period, E_beam the beam energy, $U_{0,\mathrm{SR}}$ the average energy loss per turn due to synchrotron radiation in the arc, and $U_{0,\mathrm{BS}}$ the average energy loss due to beamstrahlung in a single collision. Using Eq. (9), the average energy loss per collision due to beamstrahlung is given by

$$U_{0,\mathrm{BS}} = \delta_B E_\mathrm{e} \approx 0.84 \frac{r_\mathrm{e}^3 E_\mathrm{e} \gamma N_\mathrm{b}^2}{\sigma_z (\sigma_x + \sigma_y)^2} \,. \tag{15}$$

For all proposed future circular colliders, we have $U_{0,\mathrm{BS}} \ll U_{0,\mathrm{SR}}$, $\tau_{E,\mathrm{tot}} \approx \tau_{E,\mathrm{SR}}$, and $\sigma_x \gg \sigma_y$. In the following, we will assume these conditions to be fulfilled.

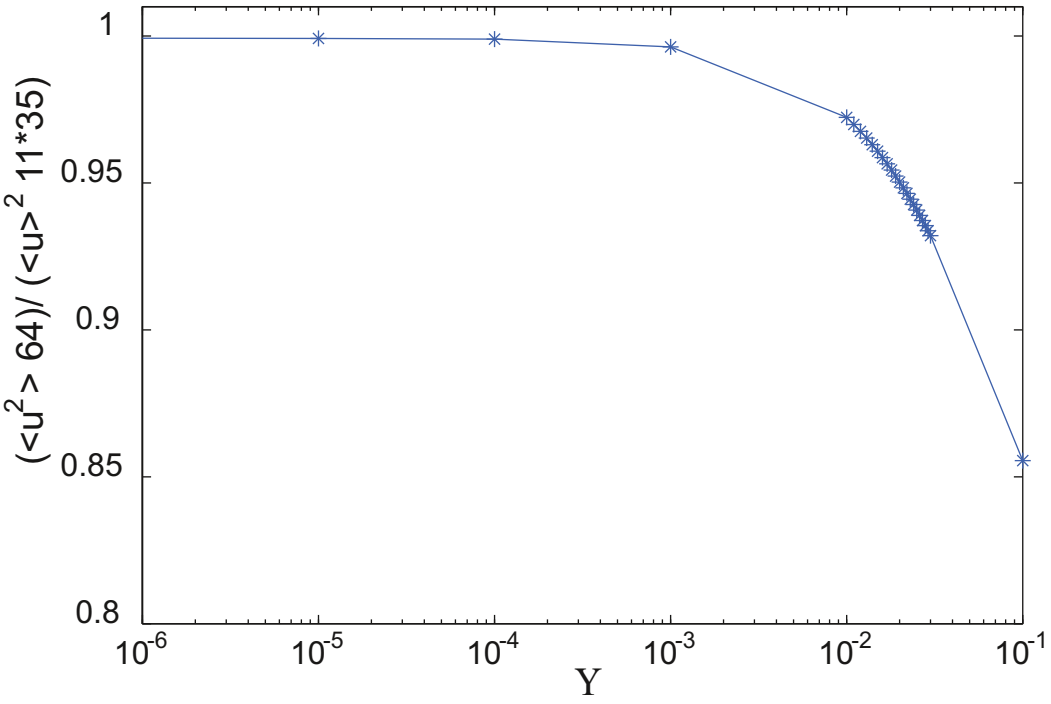

Fig. 2: Mean square photon energy normalized by the square of the mean energy according to Eq. (11) versus Υ

3.3 Self-consistent energy spread without IP dispersion

Consider first the case of zero IP dispersion. The energy spread due to the additional excitation from beamstrahlung at the collision point increases as

$$\sigma_{\mathrm{tot}}^2 = \sigma_{\delta,\mathrm{SR}}^2 + \sigma_{\delta,\mathrm{BS}}^2 \,, \tag{16}$$

with

$$\sigma_{\delta,\mathrm{BS}}^2 = \frac{n_{\mathrm{IP}}\tau_{E,\mathrm{SR}}}{4T_{\mathrm{rev}}} n_\gamma \langle u^2 \rangle \approx \frac{A}{\sigma_z^2} \,, \tag{17}$$

where the parameter A is defined as

$$A \equiv \frac{n_{\mathrm{IP}}\tau_{E,\mathrm{SR}}}{4T_{\mathrm{rev}}} n_\gamma \langle u^2 \rangle = \frac{275}{36\pi^{\frac{3}{2}}} \, \frac{n_{\mathrm{IP}}\tau_{E,\mathrm{SR}}}{4T_{\mathrm{rev}}} \frac{r_{\mathrm{e}}^5 N_{\mathrm{b}}^3 \gamma^2}{\alpha \sigma_x^3} \,. \tag{18}$$

Using the relation $\sigma_{z,\mathrm{tot}} = \sigma_{\delta,\mathrm{tot}}\sigma_{z,\mathrm{SR}}/\sigma_{\delta,\mathrm{SR}}$, self-consistency requires [18]

$$\sigma_{\delta,\mathrm{tot}}^2 - \sigma_{\delta,\mathrm{SR}}^2 = A \left(\frac{\sigma_{\delta,\mathrm{SR}}}{\sigma_{\delta,\mathrm{tot}}} \frac{1}{\sigma_{z,\mathrm{SR}}} \right)^2 \,, \tag{19}$$

where $\sigma_{z,\mathrm{SR}}$ refers to the bunch length. The energy spread $\sigma_{\delta,\mathrm{SR}}$ is computed with arc synchrotron radiation only, and the explicit solution for the total energy spread is [18]

$$\sigma_{\delta,\mathrm{tot}} = \left[\frac{1}{2}\sigma_{\delta,\mathrm{SR}}^2 + \left(\frac{1}{4}\sigma_{\delta,\mathrm{SR}}^4 + A \frac{\sigma_{\delta,\mathrm{SR}}^2}{\sigma_{z,\mathrm{SR}}^2} \right)^{1/2} \right]^{1/2} \,, \tag{20}$$

which is solved for the FCC-ee example parameters listed in Table 1, yielding the indicated values of $\sigma_{z,\mathrm{tot}}$ and $\sigma_{\delta,\mathrm{tot}}$, for the cases without monochromatization.

Table 1: Baseline beam parameters for FCC-ee crab-waist collisions at Z pole and WW threshold [4], compared with newly proposed parameters for operation on the Higgs resonance (beam energy $E_{\rm e} = 62.5\,\text{GeV}$), in simple head-on collision scheme, and with 'baseline' or 'optimized' monochromatization, for $n_{\rm IP} = 2$ identical interaction points.

$E_{\rm e}$ [GeV]	45.6	62.5	62.5	62.5	80
Scheme	Crab-waist	Head-on	Monochromatization baseline	Monochromatization optimized	Crab-waist
$I_{\rm b}$ [mA]	1450.3	408.3	408.3	408.3	151.5
$N_{\rm b}$ [10^{10}]	3.3	1.05	3.3	11.1	6.0
$n_{\rm b}$ [1]	91500	80960	25760	7728	5260
$n_{\rm IP}$ [1]	2	2	2	2	2
β_x^* [m]	1	1.0	1.0	1.96	1
β_y^* [mm]	2	2	2	1	2
D_x^* [m]	0	0	0.22	0.308	0
$\epsilon_{x,\rm SR}$ [nm]	0.09	0.17	0.17	0.17	0.26
$\epsilon_{x,\rm tot}$ [nm]	0.09	0.17	0.21	0.70	0.26
$\epsilon_{y,\rm SR}$ [pm]	1	1	1	1	1
$\sigma_{x,\rm SR}$ [μm]	9.5	9.2	132	185.7	16
$\sigma_{x,\rm tot}$ [μm]	9.5	9.2	144	188.5	16
σ_y [nm]	45	45	45	32	45
$\sigma_{z,\rm SR}$ [mm]	1.6	1.8	1.8	1.8	2.0
$\sigma_{z,\rm tot}$ [mm]	3.8	1.8	1.8	1.8	3.1
$\sigma_{\delta,\rm SR}$ [%]	0.04	0.06	0.06	0.06	0.07
$\sigma_{\delta,\rm tot}$ [%]	0.09	0.06	0.06	0.06	0.10
$\theta_{\rm c}$ [mrad]	30	0	0	0	30
circ. C [km]	100	100	100	100	100
$\alpha_{\rm C}$ [10^{-6}]	7	7	7	7	7
$f_{\rm rf}$ [MHz]	400	400	400	400	400
$V_{\rm rf}$ [GV]	0.2	0.4	0.4	0.4	0.8
$U_{0,\rm SR}$ [GeV]	0.03	0.12	0.12	0.12	0.33
$U_{0,\rm BS}$ [MeV]	0.5	0.05	0.01	0.01	0.21
$\tau_E/T_{\rm rev}$	1320	509	509	509	243
$Q_{\rm s}$	0.025	0.030	0.030	0.030	0.037
$\Upsilon_{\rm max}$ [10^{-4}]	1.7	0.8	0.3	0.85	4.0
$\Upsilon_{\rm ave}$ [10^{-4}]	0.7	0.3	0.1	0.35	1.7
$\theta_{\rm c}$ [mrad]	30	0	0	0	30
ξ_x [10^{-2}]	5	12	1	2.22	7
ξ_y [10^{-2}]	13	15	4	6.76	16
λ [1]	1	1	9.2	5.08	1
L [$10^{35}\text{cm}^{-2}\text{s}^{-1}$]	9.0	2.2	1.0	3.74	1.9
σ_w [MeV]	58	53	5.8	10.44	113

3.4 Self-consistent emittance

In the presence of non-zero dispersion at the IP, not only the energy spread, but also the transverse emittance increases due to the beamstrahlung. The non-zero dispersion may arise either from optics errors or by design, e.g., for a monochromatization scheme [19]. Under these conditions, the dynamics is similar to the well-known effect of horizontal dispersion and conventional synchrotron radiation in the storage ring arcs. The total emittance becomes

$$\epsilon_{x,\mathrm{tot}} = \epsilon_{x,\mathrm{SR}} + \frac{\tau_x n_{\mathrm{IP}}}{4T_{\mathrm{rev}}}\{n_\gamma\langle u^2\rangle\}\mathcal{H}_x^* \ , \tag{21}$$

where τ_x denotes the horizontal (amplitude) damping time due to synchrotron radiation. The non-zero dispersion invariant $\mathcal{H}_x^*$ [17] is given by

$$\mathcal{H}_x^* \equiv \frac{\left(\beta_x^* D_x'^* + \alpha_x^* D_x^*\right)^2 + D_x^{*2}}{\beta_x^*} \ , \tag{22}$$

and β_x^*, α_x^*, D_x^*, and $D_x'^*$ denote the optical beta and alpha functions (Twiss parameters), the dispersion, and the slope of the dispersion at the collision point, respectively.

The relative momentum spread is described by

$$\sigma_{\delta,\mathrm{tot}}^2 = \sigma_{\delta,\mathrm{SR}}^2 + \frac{n_{\mathrm{IP}}\tau_{E,\mathrm{SR}}}{4T_{\mathrm{rev}}}\left\{n_\gamma\langle u^2\rangle\right\} \ , \tag{23}$$

where the bunch length, appearing in Eq. (13), is related to the energy spread via [17]

$$\sigma_{z,\mathrm{tot}} = \frac{\alpha_{\mathrm{C}} C}{2\pi Q_{\mathrm{s}}}\sigma_{\delta,\mathrm{tot}} \ , \tag{24}$$

with α_{C} the momentum compaction factor, C the circumference, and Q_{s} the synchrotron tune.

Equations (21) and (23) are coupled through the excitation term $n_\gamma\langle u^2\rangle$ (Eq. (13)), leading to the formulation of a set of equations for the longitudinal and transverse plane, which must be solved self-consistently for the two unknowns σ_x and σ_z.

Simplified solutions can be obtained depending on whether $D_x^*\sigma_{\delta,\mathrm{tot}} \ll \sqrt{\beta_x^*\epsilon_x}$ (as usual for zero dispersion), or $D_x^*\sigma_{\delta,\mathrm{tot}} \gg \sqrt{\beta_x^*\epsilon_x}$ (monochromatization).

In the monochromatization approximation, $\tau_x = 2\tau_E$; using Eq. (13), Eqs. (21) and (23) can be rewritten as

$$\epsilon_{x,\mathrm{tot}} \approx \epsilon_{x,\mathrm{SR}} + \frac{2B\mathcal{H}_x^*}{D_x^{*3}\sigma_{\delta,\mathrm{tot}}^5} \ , \tag{25}$$

$$\sigma_{\delta,\mathrm{tot}}^2 = \sigma_{\delta,\mathrm{SR}}^2 + \frac{B}{D_x^{*3}\sigma_{\delta,\mathrm{tot}}^5} \ , \tag{26}$$

with

$$B \equiv 48\ \frac{n_{\mathrm{IP}}\tau_{E,\mathrm{SR}}}{T_{\mathrm{rev}}}\ \frac{r_{\mathrm{e}}^5 N_{\mathrm{b}}^3\gamma^2}{\left(\alpha_{\mathrm{C}}C/(2\pi Q_{\mathrm{s}})\right)^2} \ . \tag{27}$$

After solving Eq. (26) for the relative energy spread $\sigma_{\delta,\mathrm{tot}}$, the emittance follows from Eq. (25). Using Eqs. (26) and (25), we obtain the total bunch length and emittance for the two cases of $D_x^* \neq 0$ (the second and third column) at 62.5 GeV in Table 1. In the standard limit, i.e., the opposite case, we find

$$\epsilon_{x,\mathrm{tot}} \approx \epsilon_{x,\mathrm{SR}} + \frac{2B\mathcal{H}_x^*}{\sigma_{\delta,\mathrm{tot}}^2\beta_x^{*3/2}\epsilon_{x,\mathrm{tot}}^{3/2}} \ , \tag{28}$$

$$\sigma_{\delta,\mathrm{tot}}^2 = \sigma_{\delta,\mathrm{SR}}^2 + \frac{B}{\sigma_{\delta,\mathrm{tot}}^2 \beta_x^{*3/2} \epsilon_{x,\mathrm{tot}}^{3/2}} \ . \tag{29}$$

Equations (28) and (29) are coupled, and must be solved together. Equations (28) and (29) then yield the total bunch length and emittance shown in Table 1 for the three columns with $D_x^* = 0$.

The bunch length always follows from Eq. (24).

4 Baseline monochromatization

In a classical monochromatization scheme, with fixed emittance, energy spread, IP beta function, and only adding opposite IP dispersion for the two beams, the resulting luminosity L scales as λ^{-1}. However, for the FCC-ee, owing to the beamstrahlung in the presence of non-zero dispersion, changes in the horizontal equilibrium emittance are not negligible. A self-consistent calculation of the beam parameters then determines the actual luminosity, which tends to be less than the corresponding standard value. Moreover, the monochromatization factor deviates naively from the value expected, without taking into account the effect of the changing horizontal emittance. The self-consistent parameters must be used to compute the true values of λ and L .

Table 1 presents the nominal FCC-ee parameters for (non-monochromatic) collisions at 45.6 GeV and 80 GeV [4], with an interpolated head-on collision scheme at 62.5 GeV, a 'baseline monochromatization scheme' at the same energy (obtained by adding IP dispersion to the former), and an optimized monochromatization, for which the bunch charge and IP beta functions have been re-optimized (plus the value of the IP dispersion in proportion to $\sqrt{\beta_x^*}$).

Given the resonance width of the standard model Higgs of 4.2 MeV and the much larger natural r.m.s. energy spread of the electron and positron beams at 62.5 GeV of about 40 MeV, the monochromatization factor should be large, at least $\lambda \sim 5$ [20].

Requesting $\lambda \sim 10$, to have some margin, while considering the emittance and energy spread due to arc synchrotron radiation alone, from Table 1, the necessary value of the IP dispersion is given by $D_x^{*^2} \beta_x^{*-1} \approx 10^{-2}$ m. Using this value, the baseline monochromatization scheme in the second 62.5 GeV column of Table 1 was obtained from the first column. The value includes the effect of beamstrahlung [21].

5 Optimized monochromatization

The smaller the horizontal beta function can be made, the smaller the horizontal beam size becomes, and the smaller the luminosity loss compared with a zero-dispersion collision. As long as the resulting horizontal beam size with monochromatization, dominated by the dispersion, is much larger than the corresponding beam size for a standard collision scheme, the effects of beamstrahlung are small, at least in the longitudinal plane [21].

In an attempt to profit from the larger horizontal beam size, we may tentatively modify the bunch charge N_b (along with the number of bunches n_b) and the IP beta functions, until we reach the maximum luminosity for the selected value of λ.

For operation on the *Z* pole and at the *WW* threshold, FCC-ee applies a crab-waist scheme with $\theta_\mathrm{c} = 30$ mrad full horizontal crossing angle. The crossing angle also reduces the beam–beam tune shift, especially in the horizontal plane.

For our dispersion-based monochromatization scheme, we may need to avoid the crossing angle and (effectively) operate with head-on collisions. For head-on collisions, the beam–beam parameters (almost equal to the beam–beam tune shifts) are:

$$\xi_{x,y} = \frac{\beta_{x,y}^* r_\mathrm{e} N_\mathrm{b}}{2\pi\gamma\sigma_{x,y}(\sigma_x + \sigma_y)} \ . \tag{30}$$

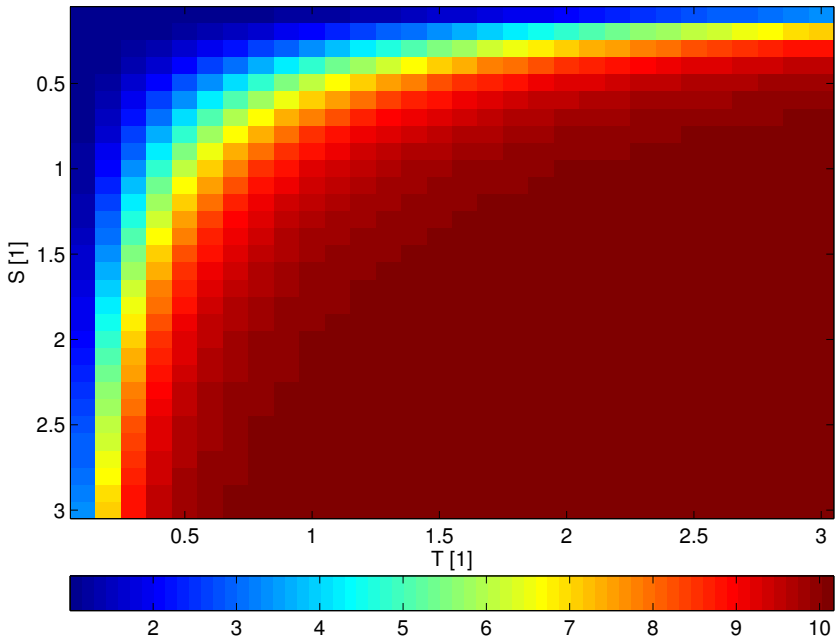

Fig. 3: λ including beamstrahlung effects

Assuming monochromatization, this can be rewritten as

$$\xi_x \approx \frac{\beta_x^* r_\mathrm{e} N_\mathrm{b}}{2\pi\gamma\sigma_\delta^2 D_x^{*2}} \,, \qquad \xi_y \approx \frac{\beta_y^* r_\mathrm{e} N_\mathrm{b}}{2\pi\gamma\sigma_\delta D_x^* \sigma_y^*} \,. \tag{31}$$

Through the constant value of the total current (limited by the synchrotron radiation power), the bunch population also defines the number of bunches per beam, n_b, and the overall luminosity

$$L \approx \frac{f_\mathrm{rev} n_\mathrm{b} N_\mathrm{b}^2}{4\pi\sigma_y^* D_x^* \sigma_\delta} \approx \frac{I_\mathrm{b}\gamma}{2e r_\mathrm{e}} \frac{\xi_y}{\beta_y^*} \,, \tag{32}$$

where f_rev denotes the revolution frequency (3 kHz).

Horizontal emittance and energy spread are normally determined by the optical lattice and the synchrotron radiation in the collider arcs. However, in the FCC-ee, the transverse effect of beamstrahlung may not always be neglected. This can be seen in Table 1, which shows horizontal emittance and beam sizes first without and then with the effect of beamstrahlung [21].

Searching for an optimal point in solution space, we reduce β_y^* from the nominal value of 2 mm to 1 mm, which is permitted by the present collider optics [22]. We then apply the following parametric transformation with parameter S (keeping λ without beamstrahlung fixed): $D_x = S * D_{ox}$, starting from $D_{ox} = 0.22$ m, and $\beta_x = S^2 * \beta_{ox}$, starting from $\beta_{ox} = 1.0$ m. We introduce a second parametric transformation with parameter T (ideally making $L \propto T^{-1}$, for the case of no beamstrahlung and no limit on the beam–beam tune shift): $n_\mathrm{b} = n_{ob} * T$ and $N_\mathrm{b} = N_{ob}/T$, so that the total beam current is constant. All initial values for D_{ox}, β_{ox}, n_{ob}, and N_{ob} correspond to the parameters of the baseline scheme, where $\lambda_\mathrm{SR} \approx 10$ (we here use λ_SR to denote the value of λ computed without the effect of beamstrahlung). The actual monochromatization factor is reduced and no longer constant in (S, T) parameter space when the effects of beamstrahlung are included, as illustrated in Fig. 3.

Under the aforementioned conditions and assumptions, including the beamstrahlung effects, the dependencies $L(\epsilon_{x,\mathrm{tot}}(T, S))$ and $\lambda(\epsilon_{x,\mathrm{tot}}(T, S))$ are analysed simultaneously. This allows determination of the maximum luminosity that can be achieved for a given λ. The result is displayed in Fig. 4.

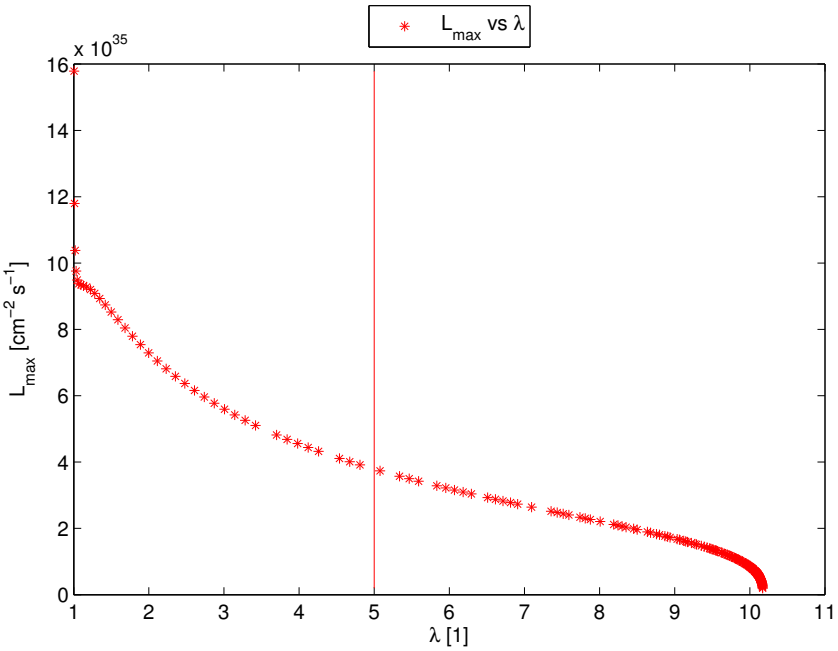

Fig. 4: Optimal luminosity as a function of λ

From this, we obtain a luminosity of $L = 3.74 \times 10^{35}$ cm^{-2}s^{-1} at $\lambda \approx 5$ (5.08), with the IP optics parameters $\beta = 4.41$ m and $D_x = 0.462$ m.

6 Conclusions and outlook

We have derived FCC-ee IP beam parameters that would result in monochromatization by a factor of 5 to 10 at high luminosity. Accounting for the horizontal increase due to beamstrahlung and non-zero IP dispersion, for a baseline monochromatization scheme a luminosity of about 10^{35} cm^{-2}s^{-1} can be achieved at the Higgs resonance with an effective collision energy spread below 6 MeV. Beamstrahlung effects lead to large horizontal increase and a concomitant degradation of the monochromatization. Nevertheless, by increasing the number of bunches, reducing the bunch charge, and increasing the optical function in the horizontal plane, beamstrahlung can be kept under control. Doing so, and keeping the beam current the same as for the baseline monochromatization, for the minimum required monochromatization of $\lambda \approx 5$ (about 10 MeV r.m.s. collision energy spread) our analytical expressions suggest that the luminosity can be increased to about 4×10^{35} cm^{-2}s^{-1}.

Optics and layout modification of the FCC-ee final-focus system [22] will represent the next challenge. We must develop a modified final-focus optics to generate the desired antisymmetric IP dispersion, and, at the same time, transit from a crossing angle to a head-on collision scheme. Either the additional bending magnets or electrostatic separators needed to realize the head-on collision that could be used to generate the necessary IP dispersion, or we can maintain a crossing geometry and deploy crab cavities together with horizontal IP dispersion.

7 Acknowledgements

We thank A. Faus-Golfe, J.M. Jowett, K. Oide, D. Shatilov, V. Telnov, and K. Yokoya for helpful discussions.

This work was supported in part by the European Commission under the FP7 Capacities project EuCARD-2, grant agreement 312453, and by the Mexican CONACyT 'BEAM' Programme.

References

[1] A. Renieri, Possibility of achieving very high energy resolution in e^+e^- storage rings, Frascati, Preprint INF/75/6(R) (1975).

[2] J.M. Jowett, Lattice and interaction region design for tau-charm factories, Proc. Joint US/CERN School on Particle Accelerators, Benalmadena, Spain, 1992, and CERN SL/93-23 (AP) (CERN, Geneva, 1993).

[3] http://cern.ch/fcc, accessed August 22nd 2016.

[4] J. Wenninger *et al.*, Future circular collider study hadron collider parameters, FCC-ACC-SPC-0003, Rev. 3.0, EDMS no. 1346081 (2016).

[5] D. d'Enterria *et al.*, Electron Yukawa from s-channel Higgs production at FCC-ee, FCC-ee Physics Workshop, Geneva, CERN, 2016.

[6] A.A. Avdienko *et al.*, The project of modernization of the VEPP-4 storage ring for monochromatic experiments in the energy range of Ψ and Υ mesons, Proc. 12th Intern. Conf. High Energy Accelerators, Fermilab, 1983, p. 186.

[7] K. Wille and A.W. Chao, Investigation of a monochromator scheme for SPEAR, SLAC/AP-32 (1984).

[8] Y.I. Alexahin *et al.*, Proposal on a tau-charm factory with monochromatization, Proc. 2nd European Particle Accelerator Conf., Nice, France, 1990, p. 398.

[9] M. Bassetti and J.M. Jowett, Improving the energy resolution of LEP experiments, Proc. 1987 IEEE PAC, Washington, DC, 1987, p. 115.

[10] A. Zholents, Polarized J/Ψ mesons at a tau-charm factory with a monochromator scheme, CERN SL/97-27, (CERN, Geneva, 1992).

[11] A. Faus-Golfe and J. Le Duff, *Nucl. Instrum. Methods A* **372** (1996) 6. https://doi.org/10.1016/0168-9002(95)01275-3

[12] A. Hofmann and E. Keil, LEP Note 70/86 (1978).

[13] V.E. Balakin *et al.*, Proc. 6th All Union Conf. on Charged Particle Accelerators, Dubna, 1978, p. 140.

[14] M. Bassetti *et al.*, Properties and possible uses of beam–beam synchrotron radiation, Proc. PAC, 1983, http://dx.doi.org/10.1109/tns.1983.4332754

[15] K. Yokoya, *Nucl. Instrum. Meth. A* **251** (1986) 1. https://doi.org/10.1016/0168-9002(86)91144-7

[16] K. Yokoya and P. Chen, *Lect. Notes Phys.* **400** (1992) 415. https://doi.org/10.1007/3-540-55250-2_37

[17] M. Sands, The physics of electron storage rings: an introduction, SLAC Report 121 (1970); also published in Conf. Proc. C6906161 (1969) p. 257.

[18] K. Ohmi and F. Zimmermann, FCC-ee/CepC beam–beam simulations with beamstrahlung, Proc. IPAC14, Dresden, 2014.

[19] M.A. Valdivia Garcia *et al.*, Towards a monochromatization scheme for direct Higgs production at FCC-ee, Proc. IPAC'16, Busan, Korea, 2016, p. 2434.

[20] A. Blondel, statement at FCC-ee physics vidyo meeting, 27 June 2016.

[21] M.A. Valdivia Garcia *et al.*, Effect of beamstrahlung on bunch length and emittance in future circular e^+e^- colliders, Proc. IPAC'16, Busan, Korea, 2016, p. 2438.

[22] K. Oide *et al.*, A design of beam optics for FCC-ee collider ring, Proc. IPAC'16, Busan, Korea, 2016, p. 3821.